

Research Article

# IGF2 deficiency causes mitochondrial defects in skeletal muscle

Yiyi Zhu<sup>1</sup>, Weiwei Gui<sup>2</sup>, Bowen Tan<sup>3</sup>, Ying Du<sup>2</sup>, Jiaqiang Zhou<sup>2</sup>, Fang Wu<sup>2</sup>, Hong Li<sup>2</sup> and  Xihua Lin<sup>2,4</sup>

<sup>1</sup>Department of Endocrinology, Peking Union Medical College Hospital, Peking Union Medical College, Chinese Academy of Medical Sciences, Beijing, China; <sup>2</sup>Department of Endocrinology, Sir Run Run Shaw Hospital, School of Medicine, Zhejiang University, Hangzhou, China; <sup>3</sup>Department of Clinical Medicine, College of Medicine, Zhejiang University, Hangzhou, China; <sup>4</sup>Biomedical Research Center and Key Laboratory of Biotherapy of Zhejiang Province, Sir Run Run Shaw Hospital, School of Medicine, Zhejiang University, Hangzhou, China

**Correspondence:** Xihua Lin (linxihua@zju.edu.cn)



Exercise training improves muscle fitness in many aspects, including induction of mitochondrial biogenesis and maintenance of mitochondrial dynamics. The insulin-like growth factors were recently proposed as key regulators of myogenic factors to regulate muscle development. The present study aimed to investigate the physical exercise impact on insulin-like growth factor 2 (IGF2) and analyzed its functions on skeletal muscle cells *in vitro*. Using online databases, we stated that IGF2 was relatively highly expressed in skeletal muscle cells and increased after exercise training. Then, IGF2 deficiency in myotubes from C2C12 and primary skeletal muscle cells (PMSCs) led to impaired mitochondrial function, reduced mitochondria-related protein content, and decreased mitochondrial biogenesis. Furthermore, we explored the possible regulatory pathway and found that mitochondrial regulation in skeletal muscle cells might occur through IGF2-Sirtuin 1 (SIRT1)-peroxisome proliferator-activated receptor- $\gamma$  co-activator-1 $\alpha$  (PGC1 $\alpha$ ) signaling pathway. Therefore, the present study first demonstrated the relationship between IGF2 and mitochondria in skeletal muscle.

## Introduction

Skeletal muscle plays a significant role in locomotion maintenance and metabolism. As highly dynamic organelles inside the skeletal muscle cell, mitochondria are responsible for regulating skeletal muscle's metabolic status [1]. Through oxidative phosphorylation (OXPHOS) to generate adenosine triphosphate (ATP), they provide energy for sustaining cellular functions [2]. When the body requires extra energy supply during exercise, mitochondria serve as main energy suppliers to coordinate ATP production, reactive oxygen species (ROS) production, and calcium signaling [3]. Therefore, exercise and mitochondria in skeletal muscle cells influence each other and maintain a close relationship.

The insulin-like growth factor system comprises three ligands, insulin, insulin-like growth factor-1 (IGF1) and insulin-like growth factor-2 (IGF2), as well as their binding proteins and receptors [4]. Both IGF1 and IGF2 are highly expressed in skeletal muscle, regulating skeletal muscle cells proliferation, differentiation, and hypertrophy [5]. Increasing evidence shows that IGF1 can be regarded as a physiological mitochondria regulator. Independent serum IGF1 concentrations and muscle IGF1 mRNA expression are closely associated with muscle mitochondria function [6]. Yet until recently, little was known about the mechanisms of IGF2 regulation in muscle mitochondrial function.

Based on the above-mentioned findings, we firstly profiled IGF2 expression in muscle tissue before and after exercise training. Next, we investigated IGF2 role on mitochondrial function and the underlying possible molecular mechanism in skeletal muscle cells. Herein, we demonstrated for the first time that IGF2 was essential to maintaining mitochondrial function in skeletal muscle cells.

Received: 01 February 2021  
Revised: 01 April 2021  
Accepted: 06 April 2021

Accepted Manuscript online:  
07 April 2021  
Version of Record published:  
16 April 2021

## Materials and methods

### Bioinformatics analysis

For analysis of IGF2 gene expression across muscle samples before and after exercise training, normalized microarray gene expression datasets were downloaded from the NCBI Gene Expression Omnibus (GEO) database. Differentially expressed genes analysis were carried out based on the limma R package. The cutoff was identified as follows: *P*-values <0.05.

### Mice

All animal care procedures and methods were performed following the guidelines of Animal Care Committee of Zhejiang University, and the animal work was carried out at Zhejiang University. Five C57BL/6 neonatal mice (2- to 5-day-old) were purchased from Slack Experimental Animal Center of the Chinese Academy of Sciences (Shanghai, China). After a 12-h light–dark cycle maintenance, mice body weights were measured, and they were then killed by cervical dislocation after exsanguination. After that, the muscle tissues of mice were collected.

### Isolation and culture of primary skeletal muscle cells

Primary cells were isolated from hindlimb muscles biopsies derived from neonatal mice (2–5 days of age). Muscles were minced with scissors in 1× PBS containing 100 IU/ml penicillin/streptomycin until a homogeneous mass was obtained. Muscle fragments were then dissociated enzymatically in 20 ml 0.25% trypsin containing 1% collagenase and were kept on a rotator at 37°C for 45 min. After adding 20 ml Dulbecco's modified Eagle's medium (DMEM) containing 10% fetal bovine serum (FBS), the suspension was filtrated into new 50-ml tubes. The suspension was centrifuged at 1500 rpm for 5 min and was resuspended in another 10 ml DMEM with 10% FBS. To purify the cell culture from fibroblasts present in the final cell pellet, 20 and 60% Percoll concentrations were used. Subsequently, the purified cells were transferred to a laminin-coated plate. After 1 h, the supernatant was transferred to a second laminin-coated plate. The first well was filled with DMEM with 10% FBS. Again, after 3 h, this procedure was repeated in the same way. After that, the cells were maintained at 37°C in a humidified atmosphere of 5% CO<sub>2</sub>.

### Immunofluorescence assay

After isolation of primary skeletal muscle cells (PMSCs) from neonatal mice, cells were cultured in the growth medium (DMEM containing 10% FBS and 100 IU/ml penicillin/streptomycin) for Olympus fluorescence microscope analysis. After washing twice with PBS, the cells were fixed with 4% paraformaldehyde for 20 min at room temperature. They were then washed with PBS three times and incubated with 0.3% Triton X-100 for permeabilization. After PBS washing, the slides were blocked in 5% BSA (Fdbio Science) for 1 h at room temperature. Subsequently, the slides were incubated with anti- $\alpha$ -actin antibody (Abclonal, 1:200) or anti-Desmin antibody (Abclonal, 1:200) at 4°C overnight. After removing the primary antibody by washing, the cell slides were incubated with FITC-conjugated secondary antibody (1: 500) (Life Technologies) for 1 h at room temperature. The nucleus was then counterstained with DAPI (Yeasen, China) for 5 min. After PBS washing to stop the chromogenic reaction, the slides were examined with Olympus fluorescence microscope. Immunofluorescent staining was performed three times, and representative images were presented.

### In vitro cell culture and differentiation

C2C12 myoblasts were purchased from American Type Cultures Collection (ATCC), and PMSCs were obtained from neonatal mice. They were cultured in a growth medium (DMEM containing 10% FBS and 100 IU/ml penicillin/streptomycin) at 37°C and 5% CO<sub>2</sub>. To induce differentiation, C2C12 and PMSCs were seeded in six-well plates, respectively, and after cells reached 80% confluence, the growth medium was switched into differentiation media (DMEM containing 2–5% horse serum). All the following experiments were carried out using myotubes.

### siRNA-mediated knockdown of IGF2

For gene knockdown, both C2C12 and PMSCs myotubes were grown in regular culture medium up to 50–70% confluence and then transiently transfected with IGF2 siRNA or NC siRNA (negative control scrambled) using Oligofectamine™ Transfection Reagent (Thermo Fisher Scientific) according to the manufacturer's protocol. siRNA sequences were shown as follows:

si-NC-F: GAAUUGCUCUCGGACAAUUCG

si-NC-R: CGAAUUGUCCGAGAGCAAUUC

si-mIGF2-1 (mouse)-F: GGAGCUUGUUGACACGCUUCA  
si-mIGF2-1 (mouse)-R: UGAAGCGUGUCAACAAGCUCC  
si-mIGF2-2 (mouse)-F: CUUGGACUUUGAGUCAAAUUGG  
si-mIGF2-2 (mouse)-R: GGUCGUGCCAAUACAUUUCA.

After 6 h of incubation with transfection reagent, cells were transferred to normal DMEM with 10% FBS. At 48 h after transfection, cells were analyzed with the indicated assays.

## RNA extraction and qRT-PCR assay

Total RNA was isolated from samples using TRIzol reagent (Invitrogen) following the manufacturer's protocol. The extracted total RNA was then quantified by a NanoDrop 2000 (Thermo Fisher, Waltham, MA). Reverse transcription (RT) was performed using a reverse transcription reagent kit (TaKaRa) to generate a cDNA template following the manufacturer's instructions. Real-time quantitative PCR was performed utilizing a PCR kit containing SYBR Green (TaKaRa) on a Roche LightCycler 480 PCR System. The relative mRNA expression levels were calculated using  $2^{-\Delta\Delta C_t}$  method and normalized to GAPDH mRNA as the internal control. The mitochondrial DNA (mtDNA) copy number was assessed by calculating the mitochondrial ratio to nuclear DNA. The primer sets used are listed in Supplementary Table S1.

## Western blot

Equal amount of protein (50  $\mu$ g) denatured by boiling was separated by 10% SDS/polyacrylamide gel electrophoresis, transferred to polyvinylidene difluoride membranes (Millipore) and blocked with 5% non-fat milk for 1 h at 37°C. Membranes were then incubated with high-affinity primary antibodies, including anti-rabbit-IGF2 (Abcam, 1:200), anti-rabbit-GAPDH (Abclonal, 1:000), anti-rabbit-Mitofusin2 (Abclonal, 1:500), anti-rabbit-DRP1 (Abclonal, 1:500), anti-rabbit-peroxisome proliferator-activated receptor- $\gamma$  co-activator-1 $\alpha$  (PGC1 $\alpha$ ; Abclonal, 1:500), and anti-mouse-Sirtuin 1 (SIRT1; Abcam, 1:1000) at 4°C overnight. After incubation with a peroxidase-labeled secondary antibody at 37°C for 1 h, signals were visualized using FDBio-Femto ECL (Fudebio, Hangzhou, China) and a chemiluminescence system (Bio-Rad, U.S.A.). All the data were quantified by ImageJ (Rawak Software, Inc., Germany). To detect the mitochondrial electron transport chain (ETC) subunits, total OXPHOS Rodent WB Antibody Cocktail Ab110413 was used to analyze relative levels of OXPHOS complexes in mouse mitochondria by Western blot. This OXPHOS cocktail contains five mouse mAbs, one each against CI subunit NDUFB8 (ab110242), CII-30kDa (ab14714), CIII-Core protein 2 (ab14745), CIV subunit I (ab14705) and CV  $\alpha$  subunit (ab14748) as an optimized premixed cocktail.

## Extracellular flux analysis

Cellular respiration was studied using Seahorse XFe96 extracellular flux analyzer (Seahorse Biosciences, Agilent technologies) following manufacturer recommended protocols. On the day before assay, 10000 cells per wells were seeded in assay microplates, and a sensor cartridge was hydrated in XF Calibrant at 37°C in a non-CO<sub>2</sub> incubator overnight. On the next day, the cells were incubated in 175 ml of assay medium at 37°C in a non-CO<sub>2</sub> incubator for 1 h until further use. We then prepared 10 $\times$  stocks of drugs in XF media, and final concentrations after injections were: 1.0  $\mu$ M Oligomycin, 1.0  $\mu$ M FCCP, and 0.5  $\mu$ M Rotenone/antimycin A. The plates were assayed on XFe96 analyzer to calculate oxygen consumption rate (OCR) over time after sequential addition of different drugs. After the run, XF Mito Stress Test Report Generator automatically calculated XF Cell Mito Stress Test parameters.

## Measurement of ROS production

According to the manufacturer's protocol, ROS production in mitochondria was detected using a ROS Assay Kit (S0033; Beyotime, Shanghai, China). Cells were incubated with 10  $\mu$ M DCFH-DA probes at 37°C for 20 min and washed twice with PBS to remove extracellular DCFH-DA. The cells were resuspended in PBS and were subjected to flow cytometric analysis (BD Biosciences). All the data were analyzed by FlowJo software (Treestar, U.S.A.) and were quantified by ImageJ (Rawak Software, Inc., Germany). The ROS production data were normalized to the siNC group.

## Measurement of mitochondrial membrane potential

To determine mitochondrial membrane potential, cells were stained live in a growth medium with the fluorescent probe JC-10 (Solarbio, 1:200) at 37°C for 20 min. After careful washing, the cells were resuspended in PBS and were

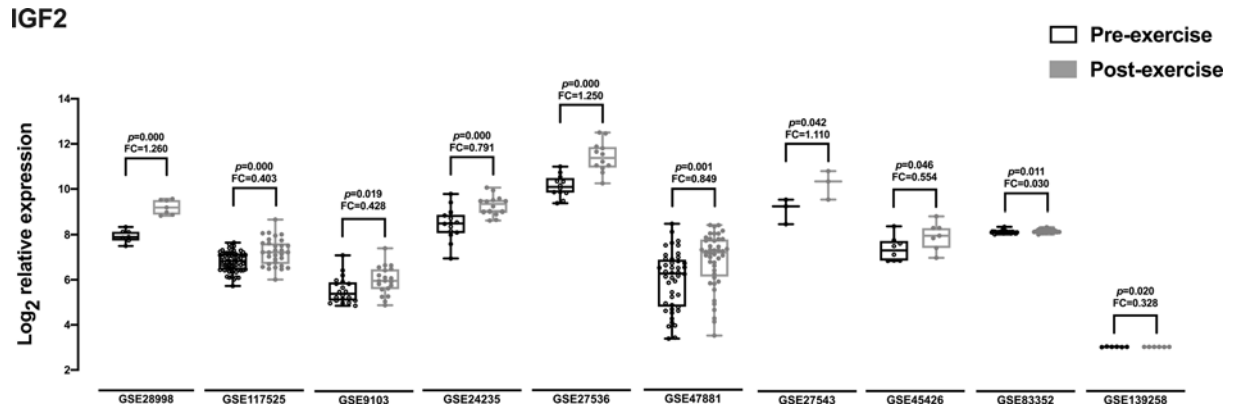


**Figure 1. Meta-analysis of microarray data comparing IGF2 gene expression in muscle tissue before and after exercise**  
Each dataset (x-axis) in the boxplot profile is noted by NCBI GEO GSE number. The y-axis indicates Log<sub>2</sub> relative expression. The blank boxes represent pre-exercise state, while the shaded boxes mean post-exercise state. *P*-values and Log<sub>2</sub> fold-change values (FC) are marked after each pairwise comparison.

subjected to flow cytometric analysis (BD Biosciences). All the data were analyzed by FlowJo software (Treestar, U.S.A.) and were quantified by ImageJ (Rawak Software, Inc., Germany). The mitochondrial membrane potential was represented as the ratio of aggregated and monomeric JC-10, and data were normalized to the siNC group.

### Transmission electron microscopy

Transmission electron microscopy (TEM) was used to determine the morphology and structure of mitochondria. Cells were fixed in 2.5% glutaraldehyde for 4 h at 4°C and post-fixed in 1% osmic acid at 37°C for 1 h. After dehydration with ethanol, the samples were transferred to absolute acetone for 20 min and embedded with 1:1 mixture of absolute acetone and embedding agent. The samples were then cut into 70 nm sections, and TEM (FEI TecnaiT10) was used to photograph mitochondria. Three randomly selected areas photographed at 5900 magnification (scale bar = 1 μm) were presented.

### MitoTracker Red staining

Cells were probed for active mitochondria by 50 nM MitoTracker Red (Invitrogen) for 30 min at 37°C in darkness, and nuclei were counterstained with DAPI (Yeasen, China) for 5 min. After washing, staining was assessed by Olympus fluorescence microscope three times, and representative images were presented.

### Statistical analysis

Data are presented as mean ± standard deviation (SD). Each experiment was performed with three biological replicates. All experiments were performed at least three times, and data were presented as means ± standard error of the mean (SEM). Statistical analysis was conducted with SPSS version 26.0 software using unpaired two-tailed Student's *t* test (normal distribution and equal variances between-group differences). The significance was represented by *P*-values and *P* < 0.05 was considered to be statistically significant, \**P* < 0.05, \*\**P* < 0.01, \*\*\**P* < 0.001, n.s., not significant.

## Results

### Differential expression profile of IGF2 in the skeletal muscle

To evaluate the expression of IGF2 among different tissues, we used the online RNA-Seq datasets from different projects. Using GTEx (<https://www.gtexportal.org/home/>), BioGPS (<http://biogps.org/>), and SAGE (<https://www.ncbi.nlm.nih.gov/geo/browse/>); these results (Supplementary Figure S1) together showed that IGF2 expression in normal human skeletal muscle tissue was relatively high. Moreover, we performed a systematic meta-analysis of microarray gene expression data and compared the relative levels of IGF2 across muscle samples before and after exercise training. Characteristics of the ten selected datasets was shown in Supplementary Table S2. Resistance or aerobic training were applied in these studies with different exercise duration from 18 days to 4 years. As shown in Figure 1, in all these studies, without exception, regardless of participants or the type and duration of exercise, IGF2 expression in

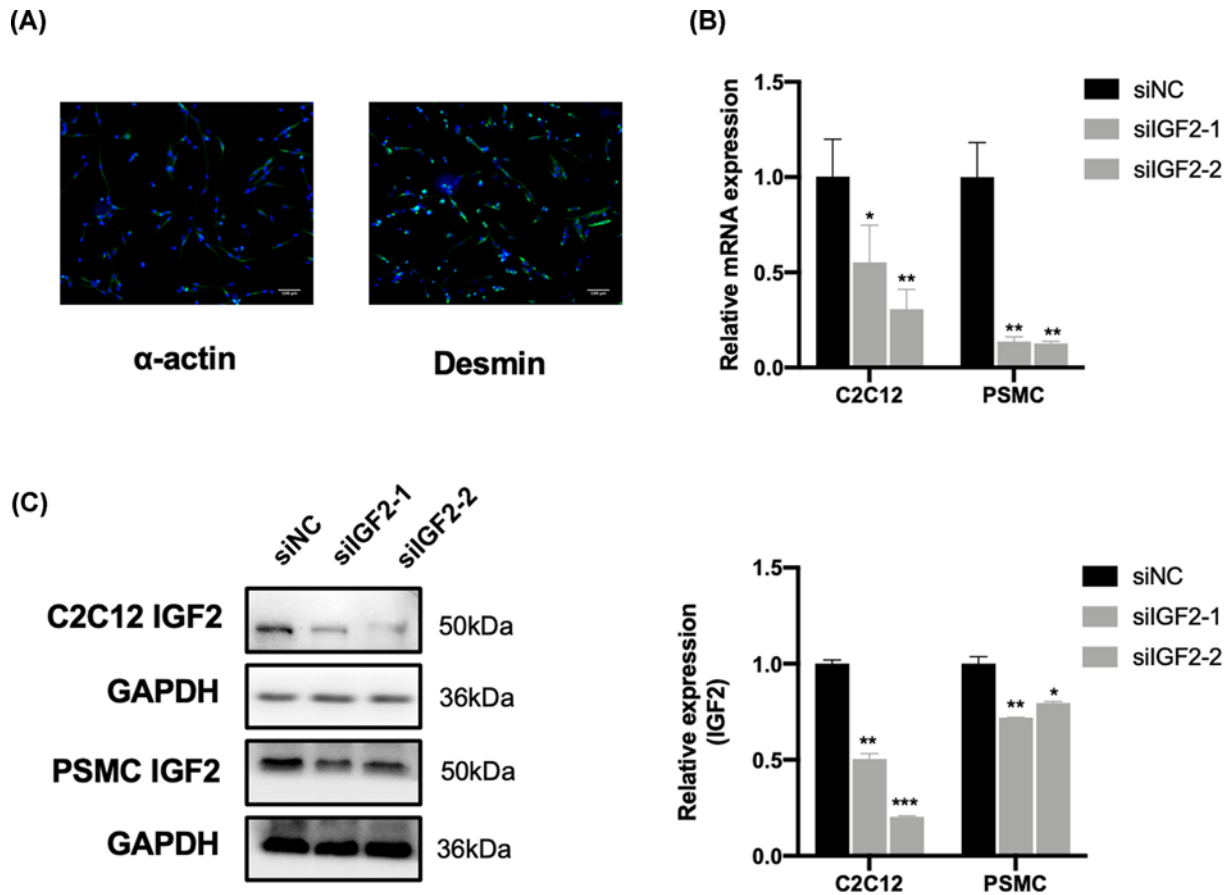


**Figure 2. Generation of IGF2 knockdown in skeletal muscle cells**

(A) Expression and distribution of  $\alpha$ -actin and Desmin in PSMCs. Scale bar = 100  $\mu$ m. The nucleus was counterstained in blue by DAPI. (B) RT-qPCR analysis validation of IGF2 knockdown in skeletal muscle cells. (C) Western blot analysis and quantification were used to demonstrate transfection efficiency in skeletal muscle cells. Data represent mean  $\pm$  SD of three biological replicates. \* $P$ <0.05, \*\* $P$ <0.01, \*\*\* $P$ <0.001.

muscle tissue increased after exercise training, and all datasets showed a highly statistically significant difference consistently. Overall, IGF2 represented a comparatively higher expression in skeletal muscle tissue and was up-regulated after exercise.

## Successful generation of IGF2-knockdown skeletal muscle cells

As skeletal muscle mitochondrial remodeling in exercise is commonly accepted [7], the alternation of IGF2 expression before and after exercise might participate in mitochondria reprogramming. In the present study, mouse C2C12 myotube and primary myotube (from PMSCs) were used as cellular models to study skeletal muscle *in vitro*.  $\alpha$ -actin and Desmin were recognized as unique proteins to characterize skeletal muscle satellite cells [8]. As demonstrated in Figure 2A, immunofluorescence results showed that  $\alpha$ -actin and Desmin stained in green were expressed in cytoplasm of PSMCs, representing that highly purified skeletal muscle satellite cells were isolated. Then, to determine IGF2 role in skeletal muscle mitochondrial function, we designed and constructed different small interfering RNAs (siRNAs) to knock down its expression in both C2C12 myotube and primary myotube. Transfection efficiency was measured by qRT-PCR and Western blot. Our findings revealed a significant over 50% down-regulation of both IGF2 mRNA and protein expression in knockdown cells, indicating that we had successfully interfered with IGF2 gene expression in these two cell lines, both  $P$ <0.05, (Figure 2B,C). Considering their transfection efficiency, we used siRNAs IGF2-2 in the following experiments.

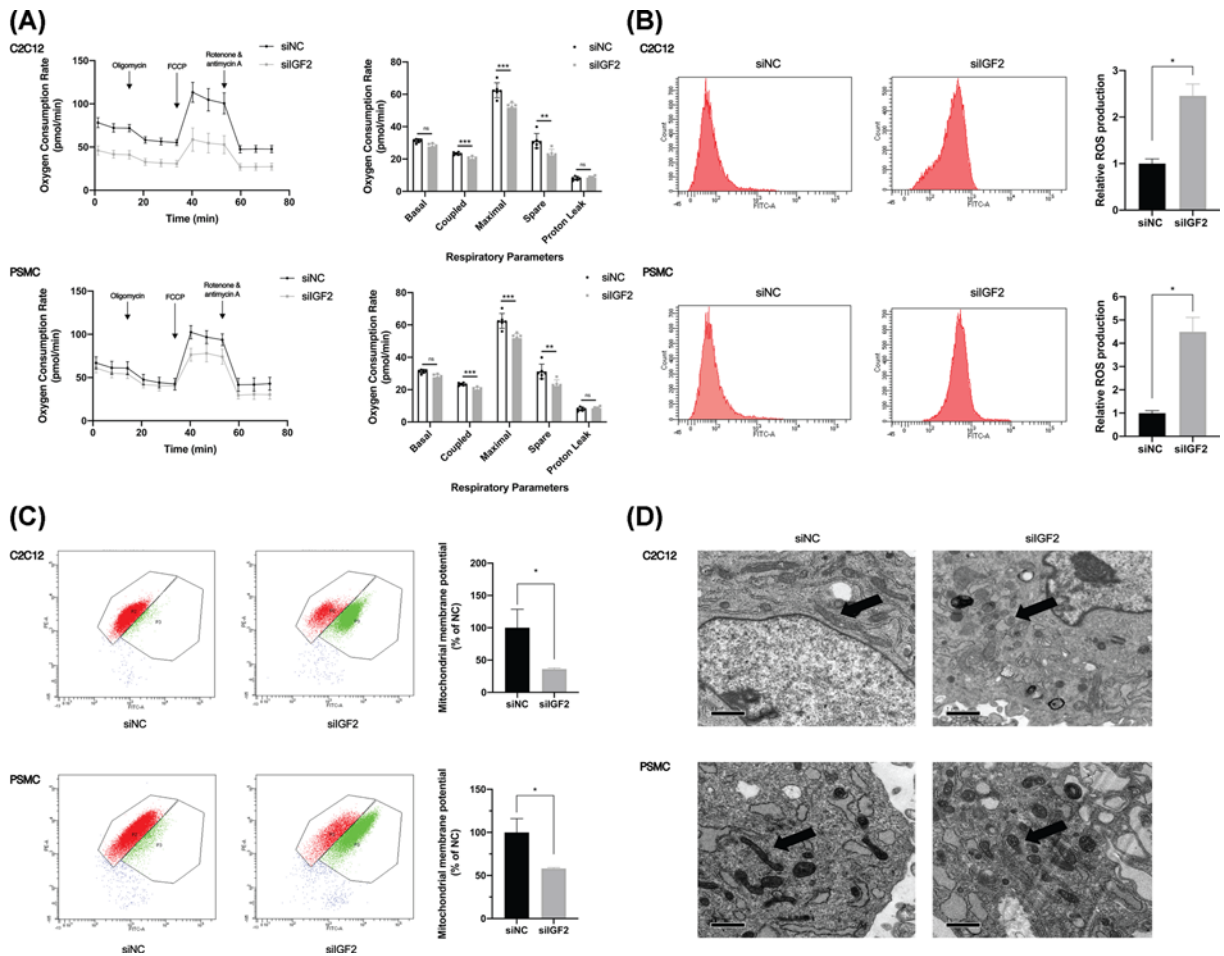


**Figure 3. Knockdown of IGF2 caused mitochondrial dysfunction in skeletal muscle cells**

(A) OCR during analysis of respiratory control in siNC and siIGF2 myotubes (left). Respiratory control parameters from siNC and siIGF2 myotubes (right). (B) ROS production was measured by flow cytometer. (C) Mitochondrial membrane potential was assessed via flow cytometer. Red fluorescence represents aggregation of JC-10, green fluorescence represents monomeric JC-10. (D) Representative electron micrographs of skeletal muscle cells from siNC and siIGF2. Scale bar = 1  $\mu$ m. Data represent mean  $\pm$  SD of three biological replicates. \* $P$ <0.05, \*\* $P$ <0.01, \*\*\* $P$ <0.001.

## Knockdown of IGF2 impaired mitochondrial function

To assess the functional impact of IGF2 loss on mitochondria, we first evaluated cellular respirometry assay using Seahorse XF96<sup>e</sup> flux analyzer on two cell lines. When comparing the respiration profiles of siNC with siIGF2 cells, we observed reduced respiration in the knockdown cells (Figure 3A). Specifically, IGF2 depletion caused a significant decline in ATP production-linked OCR, maximal respiration, and spare respiratory capacity compared with the control. Then, ROS production was assessed and displayed a significant increase after stable IGF2 knockdown, a 2.58-fold increase in C2C12 and 4.46-fold increase in PSMCs, respectively, both  $P$ <0.05, (Figure 3B). Consistently, we scrutinized the membrane potential calculated from JC-10 staining. The siIGF2 samples exhibited significant membrane depolarization, a 58.2% decrease in C2C12 and 42.6% decrease in PSMCs, respectively, both  $P$ <0.05, (Figure 3C), a strong indicator of mitochondrial dysfunction. Besides, ultrastructural findings revealed mitochondria's presence exhibiting augmented mitochondrial fission events in siIGF2 cells (Figure 3D). Compared with siNC group, there was an increased mitochondrial number and smaller mitochondrial width in siIGF2 group. As a result, we demonstrated that knockdown of IGF2 impaired mitochondrial function and remodeled the mitochondrial network (fusion and fission) in skeletal muscle cells *in vitro*.

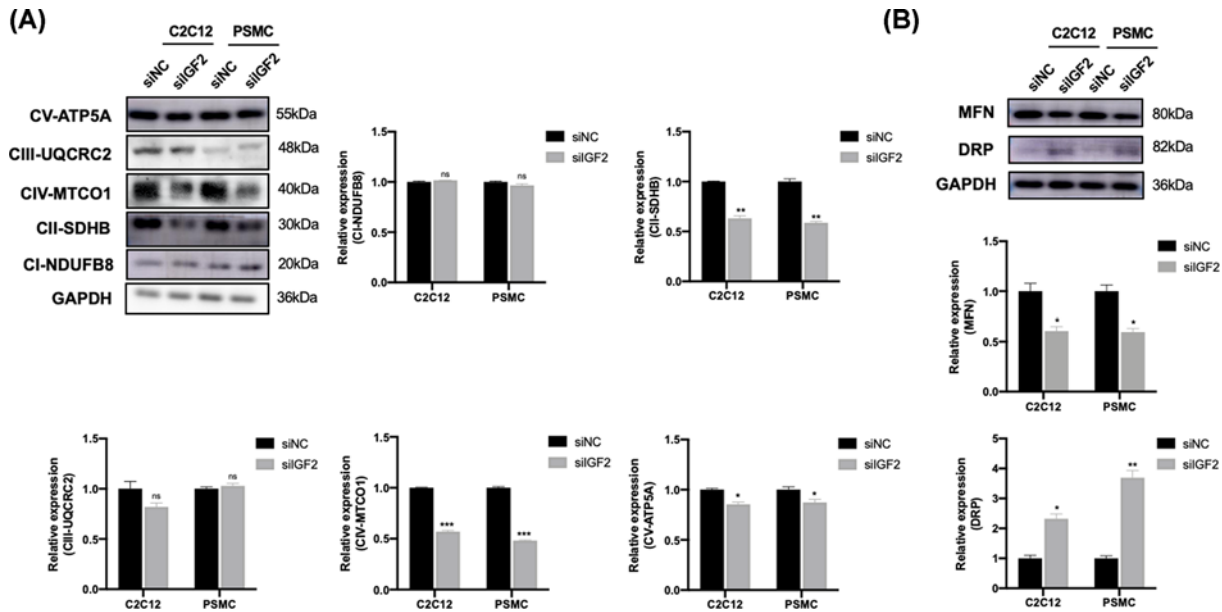


**Figure 4. Changes in markers of mitochondrial protein content in IGF2 knockdown group compared with control group**  
 (A) Protein abundance of mitochondrial subunits complex I (NDUFB8), complex II (SDHB), complex III (UQCRC2), complex IV (MTCO1), complex V (ATP5A) in siNC and siIGF2 skeletal muscle cells. (B) Effects of IGF2 knockout on the content of proteins regulating mitochondrial fusion (MFN) and fission (DRP) in siNC and siIGF2 skeletal muscle cells measured by western blot. Data represent mean  $\pm$  SD of three biological replicates. \* $P$  < 0.05, \*\* $P$  < 0.01, \*\*\* $P$  < 0.001, n.s., not significant.

## Knockdown of IGF2 impaired mitochondria-related protein content

Considering that mitochondria-related protein content expression laid the foundation for mitochondrial function and structure, we then measured the content of mitochondrial ETC subunit I–V (Figure 4A) as well as relevant mitochondrial fusion and fission proteins (Figure 4B). Mitochondrial subunits complex II (SDHB) ( $P$  < 0.01), complex IV (MTCO1) ( $P$  < 0.01) were down-regulated obviously in IGF2 knockdown cells along with a slight decrement of complex V (ATP5A) ( $P$  < 0.05). However, we did not observe a significant difference in complex I (NDUFB8) and complex III (UQCRC2) expression. Meanwhile, the siIGF2 group displayed a significantly lower level of mitochondrial fusion protein Mitofusin (MFN) ( $P$  < 0.05) and a significantly higher level of fission protein dynamic-related protein (DRP) ( $P$  < 0.05) compared with siNC group. Overall, these findings indicated that the observed decrements in mitochondrial function and fragmentation of mitochondrial structure might occur due to impaired mitochondria-related protein content.

## Knockdown of IGF2 impaired mitochondrial biogenesis

Given the observed decrement in mitochondrial respiration in IGF2 knockdown skeletal muscle cells, we sought to determine whether a reduction in mitochondrial biogenesis might underlie this phenotype. Firstly, the mitochondrial mass was assessed by mitochondrial probe staining. The results presented a reduced red fluorescence intensity in IGF2 knockdown cells, indicating a decreased mitochondrial mass after IGF2 loss (Figure 5A). mtDNA level was then measured, displaying a reduced level in IGF2 silencing cells compared with the control (Figure 5B) ( $P$  < 0.01). Consistent with the result of mtDNA content level, the transcript levels of mtDNA genes were mainly down-regulated after IGF2 knockdown (Figure 5C) ( $P$  < 0.05). In summary, these data suggested that mitochondrial biogenesis was significantly impaired in IGF2 knockdown skeletal muscle cells.

## IGF2 deficiency causes mitochondrial defects through IGF2-SIRT1-PGC1 $\alpha$ pathway

SIRT1 and PGC1 $\alpha$  enhanced mitochondrial biogenesis and energy homeostasis [9]. To test if IGF2 may regulate mitochondrial biogenesis via SIRT1-PGC1 $\alpha$  pathway, the expression of these two related proteins was detected by RT-qPCR analysis and Western blot. We stated that expression of SIRT1 and PGC-1 $\alpha$  at mRNA level was down-regulated in siIGF2 group compared with siNC group ( $P$  < 0.01, Figure 6A). Consistent with RT-qPCR analy-

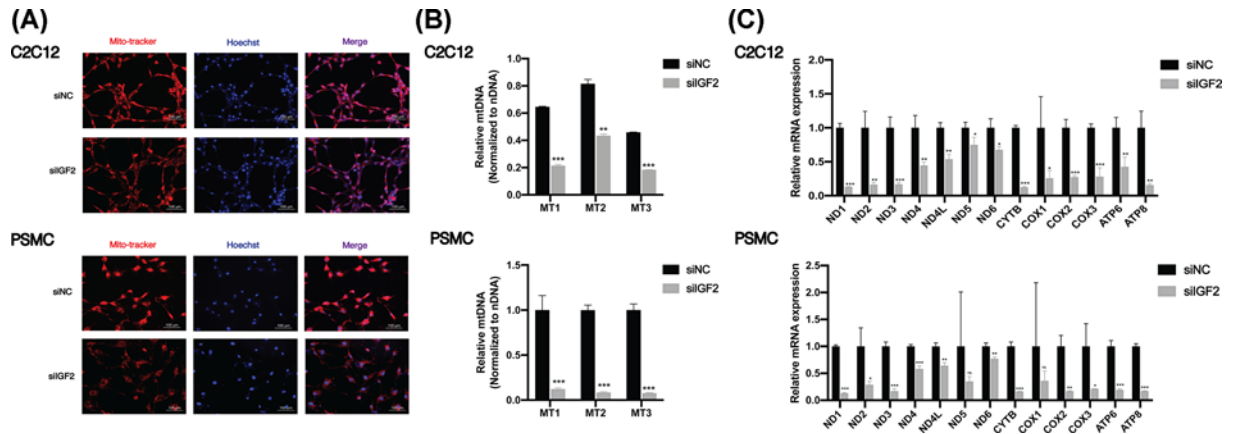


**Figure 5. Effects of IGF2 knockout on mitochondrial biogenesis in skeletal muscle cells**  
 (A) Mitochondrial mass was measured using MitoTracker staining. Scale bar = 100  $\mu$ m. (B) Relative mtDNA contents after normalization to nuclear DNA (nDNA) levels. MT1–3 represents three primers mapping to distinct regions on mtDNA. (C) mtDNA transcription levels were measured by qRT-PCR. Data represent mean  $\pm$  SD of three biological replicates. \* $P$ <0.05, \*\* $P$ <0.01, \*\*\* $P$ <0.001, n.s., not significant.

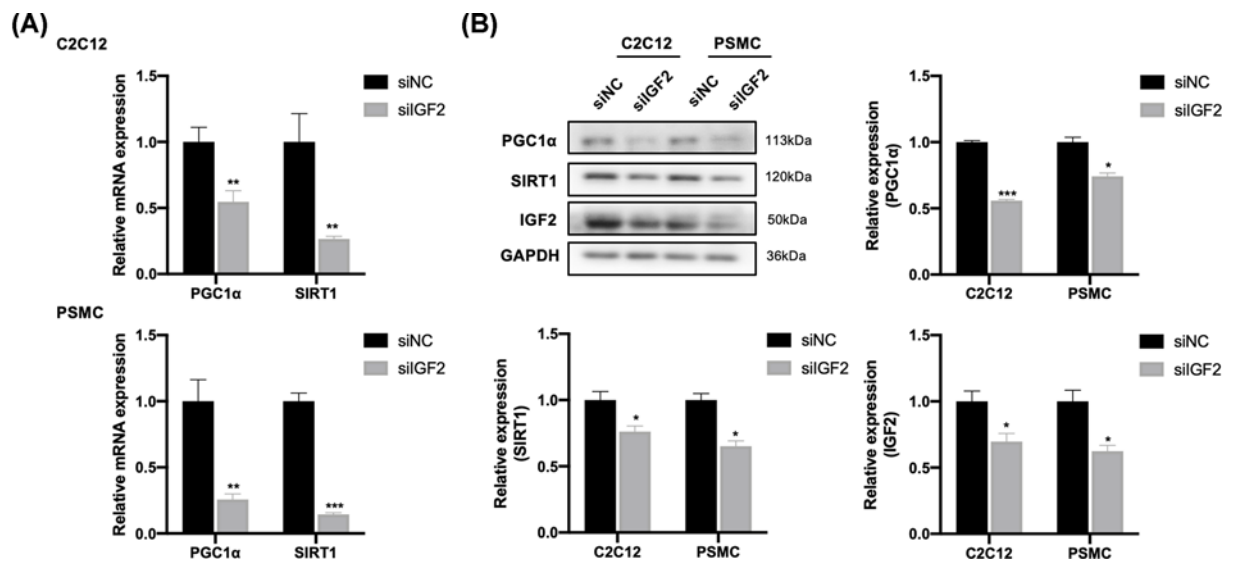


**Figure 6. Effect of IGF2 loss on mRNA and protein levels of SIRT1 and PGC-1 $\alpha$**   
 (A) The relative mRNA expression of SIRT1 and PGC-1 $\alpha$  evaluated by RT-qPCR analysis. (B) Representative images and their quantification of Western blots of SIRT1 and PGC-1 $\alpha$  protein. Data represent mean  $\pm$  SD of three biological replicates. \* $P$ <0.05, \*\* $P$ <0.01, \*\*\* $P$ <0.001.

sis results, the protein levels of SIRT1 and PGC-1 $\alpha$  were also decreased after IGF2 loss ( $P$ <0.05, Figure 6B). These data suggested that the effects of IGF2 deficiency on mitochondrial dysfunction might be through SIRT1-dependent PGC-1 $\alpha$  pathway (Figure 7).

## Discussion

IGF2 was characterized as a key quantitative trait locus for muscle enhancer [10] and was required for development and maintenance of the musculoskeletal system [11]. Younis et al. found that ZBED6–IGF2 axis regulated IGF2 expression and then affected muscle growth [12]. Moreover, Florini et al. reported that IGF2 levels increased dramatically during myogenesis in cultured muscle cells [13]. Therefore, IGF2 acted as an important regulator of myogenic growth factors in skeletal muscle cells.

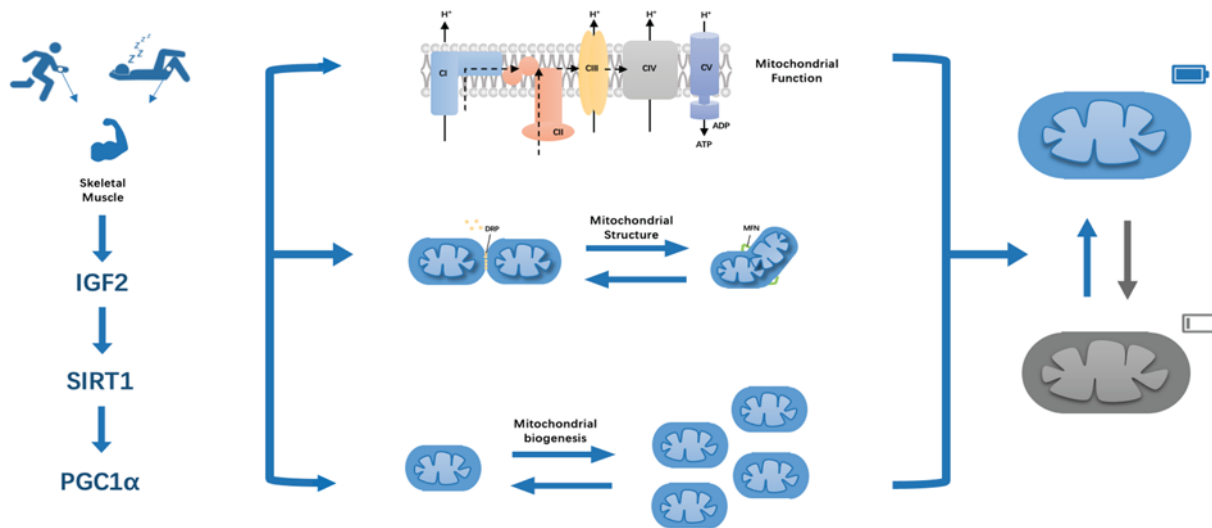


**Figure 7. Model graph proposing the potential role of IGF2 in regulating mitochondrial function in skeletal muscle**

Exercise training improves muscle fitness by induction of mitochondrial biogenesis and maintenance of mitochondrial dynamics regulated by key regulators of myogenic factors-IGF2. Knockdown of IGF2 reduced the expression of both SIRT1 and PGC-1 $\alpha$ , which might be the underlying molecular mechanism of mitochondrial dysfunction.

In this work, we explored the role and possible mechanism of IGF2 in modulating mitochondria's activity inside the skeletal muscle cells. Firstly, we identified that IGF2 expression in muscle tissues was relatively high and was altered statistically significantly before and after exercise using multiple online research data. Increasing evidence has demonstrated that mitochondrial dynamics have essential roles in maintenance of metabolism in skeletal muscle. Especially in response to exercise, mitochondria form large networks within skeletal muscle cells to meet the energy requirement [3]. Based on the previous studies, it can be inferred that IGF2 might participate in mitochondrial modulation process.

This exercise-induced adaptation resulted in positive alternations in mitochondrial function [14]. As for mitochondrial function, exercise promoted ROS loss and high mitochondrial membrane potential, leading to increased respiration function [15]. Apart from that, remodeling of mitochondrial network (fusion and fission) from exercise can also be observed to improve mitochondria's efficiency [16]. Due to the increased content of IGF2 after exercise, we speculated that IGF2 knockdown might damage mitochondria's function. As expected, IGF2 depletion caused a significant reduction in mitochondrial respiration in both C2C12 myotubes and primary myotubes, accompanied by excessive ROS generation and mitochondrial membrane potential degradation. Specifically, mitochondrial respiration state was influenced in three aspects: ATP production-linked OCR, maximal respiration, and spare respiratory capacity. This phenomenon represented that IGF2 loss had defects in the mitochondrial OXPHOS process (mtOXPHOS). The inhibition of OXPHOS lowered the mitochondrial membrane potential and triggered the relatively higher production of cellular ROS as a byproduct of oxidative phosphorylation [17].

The mtOXPHOS process occurred via protein complexes of ETC. Therefore, we performed Western blots to measure protein levels of ETC proteins and ATP synthase (complex V), where the results indicated that IGF2 knockdown specifically inhibited the levels of SDHB (a subunit of complex II), MTCO1 (a subunit of complex IV), and ATP5A (a subunit of complex V). Therefore, we reported that one possible reason for impairment observed in respiration might be the decreased expression of mitochondrial respiratory chain complexes. Also, it has been acknowledged that Complex II was one of the contributors to ROS production [18]. Our study showed a noticeable decrement of SDHB (a subunit of complex II) expression after IGF2 knockdown, representing the possible ROS source. Meanwhile, more fission events and fewer fusion events happened after IGF2 knockdown, with the imbalance of DRP/MFN expression. MFN initiated fusion by tethering adjacent mitochondria [19], while DRP mediated fission by inducing mitochondrial fragmentation [20]. The fused mitochondria were optimal for ATP generation [21], so fused mitochondria loss after IGF2 knockdown also led to a decrement of ATP generation. This might be another reason to explain the dysfunctional mitochondrial respiratory.

Mitochondrial dysfunction is also caused by impaired mitochondrial biogenesis and inhibited mtDNA transcription [22]. The results of this study showed that low IGF2 expression could reduce mitochondria number. Consistent with mitochondrial quantity reduction, mtDNA genes and their transcripts levels were globally down-regulated. Furthermore, mitochondrial biogenesis was orchestrated by PGC-1 family of transcriptional co-activators [23] and PGC-1 $\alpha$  induced OXPHOS genes involved in the final step of ETC and ATP synthesis [24]. Through PGC-1 $\alpha$  deacetylation, SIRT1 regulated the gene expression of PGC-1 $\alpha$  [9]. Here, we found that knockout of IGF2 reduced the expression of both SIRT1 and PGC-1 $\alpha$ , which might be the underlying molecular mechanism of mitochondrial dysfunction.

From the future perspective, the age-related muscle degeneration is a major concern in the aging society and the main factor is regarded as derangements in skeletal myocyte mitochondrial function. As shown in Figure 7, exercise increases the local concentration of IGF2 in skeletal muscle. As a myogenic factor, IGF2 participates in maintaining the muscle health and mitochondrial function. In contrast, loss of IGF2 breaks the balance of mitochondrial dynamics. Thus, IGF2 might be a potential therapeutic target in muscle mitochondrial dysfunction.

## Conclusion

In conclusion, we demonstrated for the first time that IGF2 expression increased after exercise training. With IGF2 knockout, mitochondria were dysfunctional in skeletal muscle cells related to a reduced content of mitochondrial-related protein, imbalance of mitochondrial fission/fusion, and impaired mitochondrial biogenesis. The potential molecular mechanism caused by mitochondrial defects may occur through IGF2-SIRT1-PGC1 $\alpha$  pathway (Figure 7).

### Clinical perspectives

- Exercise training enhances muscle fitness in numerous aspects, comprising mitochondrial biogenesis induction and mitochondrial dynamics maintenance.
- The insulin-like growth factors were recently suggested as key regulators of myogenic factors to regulate muscle development. The relationship between IGF2 and mitochondrial function in skeletal muscle cells remained unclear.
- This research intended to investigate physical exercise's impact on IGF2 and analyzed its functions and possible regulatory pathway on mitochondria in skeletal muscle cells *in vitro*.

### Data Availability

The datasets used and/or analyzed in the current study are available from the corresponding author on reasonable request.

### Competing Interests

The authors declare that there are no competing interests associated with the manuscript.

### Funding

This work was supported by the Zhejiang Provincial Medical Science Foundation of China [grant number LY20H070004]; and the Zhejiang Provincial Medical Science and Technology Program [grant numbers 2020KY166, 2018KY484].

### CRedit Author Contribution

**Yiyi Zhu:** Validation, Investigation, Methodology, Writing—review and editing. **Weiwei Gui:** Validation, Investigation, Methodology. **Bowen Tan:** Investigation, Methodology. **Ying Du:** Resources, Funding acquisition, Validation, Methodology. **Jiaqiang Zhou:** Resources, Supervision, Project administration. **Fang Wu:** Supervision, Funding acquisition, Project administration. **Hong Li:** Conceptualization, Supervision, Funding acquisition, Project administration. **Xihua Lin:** Conceptualization, Resources, Formal analysis, Supervision, Funding acquisition, Validation, Methodology, Writing—original draft, Project administration, Writing—review and editing.

## Ethics Approval

All human study and animal experiments were performed in accordance with protocols approved by the Ethics Committee of Sir Run Run Shaw Hospital, Hangzhou, Zhejiang, China.

## Abbreviations

ATP, adenosine triphosphate; DAPI, 4,6-diamino-2-phenyl indole; DMEM, dulbecco's modified eagle's medium; DCFH-DA, 2,7-dichlorodi-hydrofluorescein diacetate; DRP, dynamic-related protein; ETC, electron transport chain; FBS, fetal bovine serum; GAPDH, glyceraldehyde-3-phosphate dehydrogenase; IGF1/2, insulin-like growth factor 1/2; MFN, mitofusin; mtDNA, mitochondrial DNA; mtOXPHOS, mitochondrial oxidative phosphorylation; OCR, oxygen consumption rate; OXPHOS, oxidative phosphorylation; PGC1 $\alpha$ , peroxisome proliferator-activated receptor- $\gamma$  co-activator-1 $\alpha$ ; PMSC, primary skeletal muscle cell; qRT-PCR, quantitative real-time PCR; ROS, reactive oxygen species; siRNA, small interfering RNA; SIRT1, sirtuin 1; TEM, transmission electron microscopy.

## References

- Hood, D.A., Memme, J.M., Oliveira, A.N. and Triolo, M. (2018) Maintenance of skeletal muscle mitochondria in health, exercise, and aging. *Annu. Rev. Physiol.* **81**, 19–41, <https://doi.org/10.1146/annurev-physiol-020518-114310>
- Mitchell, P. (1961) Coupling of phosphorylation to electron and hydrogen transfer by a chemi-osmotic type of mechanism. *Nature* **191**, 144–148, <https://doi.org/10.1038/191144a0>
- Huertas, J.R., Casuso, R.A., Agustin, P.H. and Cogliati, S. (2019) Stay fit, stay young: mitochondria in movement: the role of exercise in the new mitochondrial paradigm. *Oxid. Med. Cell. Longev.* **2019**, 7058350, <https://doi.org/10.1155/2019/7058350>
- van Beijnum, J.R., Pieters, W., Nowak-Sliwinska, P. and Griffioen, A.W. (2017) Insulin-like growth factor axis targeting in cancer and tumour angiogenesis - the missing link. *Biol. Rev. Camb. Philos. Soc.* **92**, 1755–1768, <https://doi.org/10.1111/brv.12306>
- Zanou, N. and Gailly, P. (2013) Skeletal muscle hypertrophy and regeneration: interplay between the myogenic regulatory factors (MRFs) and insulin-like growth factors (IGFs) pathways. *Cell. Mol. Life Sci.* **70**, 4117–4130, <https://doi.org/10.1007/s00018-013-1330-4>
- Hamarneh, S.R., Murphy, C.A., Shih, C.W., Frontera, W., Torriani, M., Irazoqui, J.E. et al. (2015) Relationship between serum IGF-1 and skeletal muscle IGF-1 mRNA expression to phosphocreatine recovery after exercise in obese men with reduced GH. *J. Clin. Endocrinol. Metab.* **100**, 617–625, <https://doi.org/10.1210/jc.2014-2711>
- Gan, Z., Fu, T., Kelly, D.P. and Vega, R.B. (2018) Skeletal muscle mitochondrial remodeling in exercise and diseases. *Cell Res.* **28**, 969–980, <https://doi.org/10.1038/s41422-018-0078-7>
- Liu, Y., Chen, S., Li, W., Du, H. and Zhu, W. (2012) Isolation and characterization of primary skeletal muscle satellite cells from rats. *Toxicol. Mech. Methods* **22**, 721–725, <https://doi.org/10.3109/15376516.2012.720302>
- Tang, B.L. (2016) Sirt1 and the mitochondria. *Mol. Cells* **39**, 87–95, <https://doi.org/10.14348/molcells.2016.2318>
- Alzhanov, D. and Rotwein, P. (2016) Characterizing a distal muscle enhancer in the mouse Igf2 locus. *Physiol. Genomics* **48**, 167–172, <https://doi.org/10.1152/physiolgenomics.00095.2015>
- Livingstone, C. and Borai, A. (2014) Insulin-like growth factor-II: its role in metabolic and endocrine disease. *Clin. Endocrinol. (Oxf.)* **80**, 773–781, <https://doi.org/10.1111/cen.12446>
- Younis, S., Schonke, M., Massart, J., Hjortebjerg, R., Sundstrom, E., Gustafson, U. et al. (2018) The ZBED6-IGF2 axis has a major effect on growth of skeletal muscle and internal organs in placental mammals. *Proc. Natl. Acad. Sci. U.S.A.* **115**, E2048–E2057, <https://doi.org/10.1073/pnas.1719278115>
- Florini, J.R., Ewton, D.Z. and Coolican, S.A. (1996) Growth hormone and the insulin-like growth factor system in myogenesis. *Endocr. Rev.* **17**, 481–517
- Lundby, C. and Jacobs, R.A. (2016) Adaptations of skeletal muscle mitochondria to exercise training. *Exp. Physiol.* **101**, 17–22, <https://doi.org/10.1113/EP085319>
- Heden, T.D., Johnson, J.M., Ferrara, P.J., Eshima, H., Verkerke, A.R.P. and Wentzler, E.J. (2019) Mitochondrial PE potentiates respiratory enzymes to amplify skeletal muscle aerobic capacity. *Sci. Adv.* **5**, 1–11, <https://doi.org/10.1126/sciadv.aax8352>
- Axelrod, C.L., Fealy, C.E., Mulya, A. and Kirwan, J.P. (2019) Exercise training remodels human skeletal muscle mitochondrial fission and fusion machinery towards a pro-elongation phenotype. *Acta Physiol. (Oxf.)* **225**, e13216, <https://doi.org/10.1111/apha.13216>
- Mailloux, R.J., McBride, S.L. and Harper, M.E. (2013) Unearthing the secrets of mitochondrial ROS and glutathione in bioenergetics. *Trends Biochem. Sci.* **38**, 592–602, <https://doi.org/10.1016/j.tibs.2013.09.001>
- Quinlan, C.L., Orr, A.L., Perevoshchikova, I.V., Treberg, J.R., Ackrell, B.A. and Brand, M.D. (2012) Mitochondrial complex II can generate reactive oxygen species at high rates in both the forward and reverse reactions. *J. Biol. Chem.* **287**, 27255–27264, <https://doi.org/10.1074/jbc.M112.374629>
- Koshiba, T., Detmer, S.A., Kaiser, J.T., Chen, H., McCaffery, J.M. and Chan, D.C. (2004) Structural basis of mitochondrial tethering by mitofusin complexes. *Science* **305**, 858–862, <https://doi.org/10.1126/science.1099793>
- Frank, S., Gaume, B., Bergmann-Leitner, E.S., Leitner, W.W. and Robert, E.G. (2001) The role of dynamin-related protein 1, a mediator of mitochondrial fission, in apoptosis. *Dev. Cell* **1**, 515–525, [https://doi.org/10.1016/S1534-5807\(01\)00055-7](https://doi.org/10.1016/S1534-5807(01)00055-7)
- Farmer, T., Naslavsky, N. and Caplan, S. (2018) Tying trafficking to fusion and fission at the mighty mitochondria. *Traffic* **19**, 569–577, <https://doi.org/10.1111/tra.12573>

- 22 Sheng, B., Wang, X., Su, B., Lee, H.G., Casadesus, G., Perry, G. et al. (2012) Impaired mitochondrial biogenesis contributes to mitochondrial dysfunction in Alzheimer's disease. *J. Neurochem.* **120**, 419–429, <https://doi.org/10.1111/j.1471-4159.2011.07581.x>
- 23 Scarpulla, R.C. (2008) Transcriptional paradigms in mammalian mitochondrial biogenesis and function. *Physiol. Rev.* **88**, 611–638, <https://doi.org/10.1152/physrev.00025.2007>
- 24 Ruas, J.L., White, J.P., Rao, R.R., Kleiner, S., Brannan, K.T., Harrison, B.C. et al. (2012) A PGC-1alpha isoform induced by resistance training regulates skeletal muscle hypertrophy. *Cell* **151**, 1319–1331, <https://doi.org/10.1016/j.cell.2012.10.050>